

Hyperentangled Bell-state analysis and hyperdense coding assisted by auxiliary entanglement

Xi-Han Li^{1,2,*} and Shohini Ghose^{2,3,4}

¹*Department of Physics, Chongqing University, Chongqing, China*

²*Department of Physics and Computer Science, Wilfrid Laurier University, Waterloo, Canada*

³*Institute for Quantum Computing, University of Waterloo, Waterloo, Canada*

⁴*Perimeter Institute for Theoretical Physics, Waterloo, Canada*

(Received 20 June 2017; published 21 August 2017)

We present a technique for hyperentangled Bell-state analysis that only relies on linear optics and is assisted by auxiliary entangled states. This technique can be used to implement hyperdense coding with an experimentally realizable two-photon state hyperentangled in polarization and two longitudinal-momentum degrees of freedom. The 16 hyperentangled states in the first two degrees of freedom are classified into 12 groups with the help of the third degree of freedom. This allows the transmission of 3.58 bits/photon via our hyperdense coding scheme. We also generalize our technique to n -qubit hyperentangled Bell-state analysis assisted by additional auxiliary entangled states. We show that given n degrees of freedom, the 4^n hyperentangled Bell states can be separated via linear optics into $x_k = 2^{n+k+1} - 2^{2k}$ groups with the help of k ($k \leq n$) ancillary entangled states. When $k = n$, all 4^n hyperentangled states can be distinguished. Our results are useful for quantum information processing based on hyperentanglement.

DOI: [10.1103/PhysRevA.96.020303](https://doi.org/10.1103/PhysRevA.96.020303)

I. INTRODUCTION

Quantum entanglement is a counterintuitive phenomenon and a key quantum resource that enables computation and communication unimaginable in the classical world. It has extensive applications in quantum information processing, including quantum teleportation [1], quantum dense coding [2,3], entanglement swapping [4], quantum repeaters [5], and other such tasks. In quantum dense coding, a two-qubit entangled Bell state is used to transmit two bits of classical information by sending just one qubit. Furthermore, particles entangled in multiple dimensions or multiple degrees of freedom (DOFs) can achieve higher information transmission rates. The so-called hyperentangled state [6–8], which is simultaneously entangled in more than one DOF, has attracted much attention recently, not only because it can improve both channel capacity and security, but also due to its use for conventional Bell-state analysis (BSA).

In many quantum information processing protocols, entangled state analysis is an important part of the protocol. For example, the discrimination of the four Bell states is essential in quantum teleportation, quantum dense coding, and entanglement swapping. However, although these states are mutually orthogonal and should be unambiguously distinguishable, they are difficult to differentiate with current technology [9–13]. The Bell states can only be separated into three groups via linear optics and only two of the four states can be identified. The problem is even more challenging for multipartite entangled states, multidimensional entangled states, and hyperentangled states. Complete BSA can be accomplished by resorting to additional resources, such as nonlinear interactions or an enlarged Hilbert space [14–19]. Similarly, hyperentangled Bell-state analysis (HBSA) can also be achieved with the help of nonlinear interactions [20–24]. However, complete HBSA is impossible with linear optics alone. It has been shown that 16 two-DOF hyperentangled

Bell states can be grouped into seven classes [25], with which the classical information sent in hyperdense coding can be up to 2.81 bits/photon [26]. Moreover, for states entangled in n DOFs, at most $2^{n+1} - 1$ groups out of 4^n hyperentangled Bell states can be distinguished by linear evolution and local projective measurements [27]. In these two schemes, each group contains more than one state when n is larger than one. In other words, none of these states can be unambiguously identified. Therefore, this hyperentangled Bell-state analysis scheme is not useful for tasks such as quantum teleportation.

In this Rapid Communication, we present a method for HBSA that uses auxiliary entangled states and can be implemented with linear optics, avoiding nonlinear interactions. The ancillary entangled states are encoded in additional DOFs of the two originally entangled photons. We apply our method to propose a practical quantum hyperdense coding scheme using a two-photon six-qubit hyperentangled state that has been experimentally realized. The two photons are entangled in the polarization and two longitudinal-momentum DOFs at the same time. We show that the 16 hyperentangled states in the first and second DOFs can be divided into 12 groups assisted by the entanglement in the third DOF. In this case, 3.58 bits of information can be transmitted by sending one photon. Moreover, eight of the 16 states can be unambiguously identified with our protocol. We also discuss HBSA assisted by auxiliary entanglement more generally. We find that for n -qubitlike DOFs, the 4^n hyperentangled Bell states can be grouped into $x_k = 2^{n+k+1} - 2^{2k}$ classes with the help of k auxiliary entangled states. Thus, when $k = n$, complete HBSA can be achieved. Our results are useful for current quantum information processing schemes based on hyperentangled Bell states, and also provide guidelines and different avenues for designing future tasks.

II. HYPERDENSE CODING VIA LINEAR OPTICS

In 2009, a six-qubit hyperentangled state was realized by entangling two photons in three DOFs—the polarization DOF

*xihanlicqu@gmail.com

and two longitudinal momentum DOFs [8]. Here, we use this experimentally available hyperentangled state to implement a hyperdense coding scheme based on our HBSA technique. A two-photon six-qubit hyperentangled Bell state can be written as

$$\begin{aligned}
 |\Upsilon\rangle_{AB} &= \frac{1}{\sqrt{2}}(|H\rangle_A|H\rangle_B + |V\rangle_A|V\rangle_B) \\
 &\otimes \frac{1}{\sqrt{2}}(|I\rangle_A|I\rangle_B + |E\rangle_A|E\rangle_B) \\
 &\otimes \frac{1}{\sqrt{2}}(|l\rangle_A|r\rangle_B + |r\rangle_A|l\rangle_B). \quad (1)
 \end{aligned}$$

A and B represent the two hyperentangled photons. H and V are the horizontal and vertical polarization states. $I(l)$ and $E(r)$ are the bases of the first (second) linear momentum, referring to “internal (left)” and “external (right)” states, respectively. Here, we have adopted the notation in Ref. [8] for simplicity. The four Bell states in the polarization DOF are

$$\begin{aligned}
 |\Phi^\pm\rangle &\equiv \frac{1}{\sqrt{2}}(|HH\rangle \pm |VV\rangle)_{AB}, \\
 |\Psi^\pm\rangle &\equiv \frac{1}{\sqrt{2}}(|HV\rangle \pm |VH\rangle)_{AB}, \quad (2)
 \end{aligned}$$

and the four Bell states in the first momentum DOF are

$$\begin{aligned}
 |\phi^\pm\rangle &\equiv \frac{1}{\sqrt{2}}(|II\rangle \pm |EE\rangle)_{AB}, \\
 |\psi^\pm\rangle &\equiv \frac{1}{\sqrt{2}}(|IE\rangle \pm |EI\rangle)_{AB}. \quad (3)
 \end{aligned}$$

In our hyperdense coding scheme, only the first and second DOFs are utilized to carry information. The third DOF is set to a fixed entangled state $|\varphi^+\rangle = \frac{1}{\sqrt{2}}(|lr\rangle + |rl\rangle)_{AB}$, which assists the HBSA in the first and second DOFs.

Our hyperdense coding protocol can be accomplished via the following steps:

(1) The receiver Bob prepares a hyperentangled state $|\Upsilon\rangle_{AB}$, and then sends the photon A to the sender Alice through a quantum channel.

(2) After receiving the photon A , Alice performs one of the 16 unitary operations $U_{ij} = \sigma_i \otimes \sigma'_j$ ($i, j = 0, 1, 2, 3$) on the photon A . Here, σ_i is one of the four operations on the polarization state,

$$\begin{aligned}
 \sigma_0 &= |H\rangle\langle H| + |V\rangle\langle V|, & \sigma_1 &= |H\rangle\langle H| - |V\rangle\langle V|, \\
 \sigma_2 &= |V\rangle\langle H| + |H\rangle\langle V|, & \sigma_3 &= |V\rangle\langle H| - |H\rangle\langle V|, \quad (4)
 \end{aligned}$$

and σ'_j is one of the following operations on the first longitudinal-momentum DOF,

$$\begin{aligned}
 \sigma'_0 &= |I\rangle\langle I| + |E\rangle\langle E|, & \sigma'_1 &= |I\rangle\langle I| - |E\rangle\langle E|, \\
 \sigma'_2 &= |E\rangle\langle I| + |I\rangle\langle E|, & \sigma'_3 &= |E\rangle\langle I| - |I\rangle\langle E|. \quad (5)
 \end{aligned}$$

These operations can be easily accomplished by linear optics. Then Alice sends A back to Bob.

(3) Bob performs HBSA on the two photons to read Alice's information encoded by her operations. His setup is shown in Fig. 1. The polarizing beam splitter (PBS) at 0° transmits horizontal polarization and reflects vertical polarization. The 50:50 beam splitters (BSs) convert incident spatial modes as $A \rightarrow$

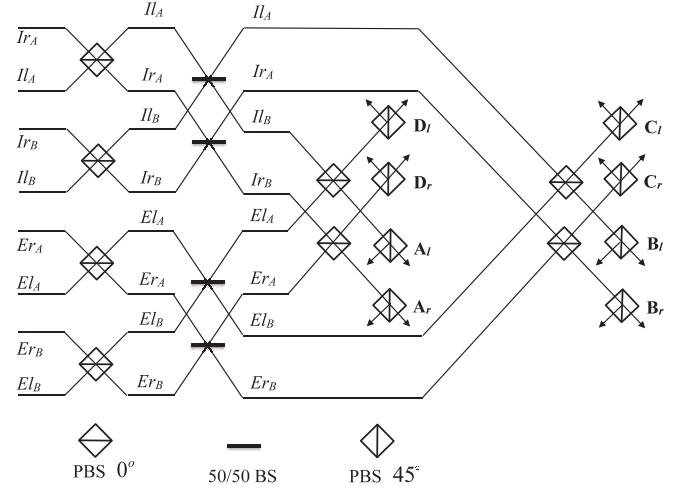


FIG. 1. Schematic of the setup for HBSA of two DOFs when photons are entangled in three DOF.

$(A + B)/\sqrt{2}$, $B \rightarrow (A - B)/\sqrt{2}$. Here, we use $A(B)$ to represent the corresponding channel photon $A(B)$ goes through. Finally, the photons are measured in the diagonal basis of the polarization DOF. The PBS orientated at 45° transmits $|+\rangle = (|H\rangle + |V\rangle)/\sqrt{2}$ and reflects $|-\rangle = (|H\rangle - |V\rangle)/\sqrt{2}$. For example, the state $\Psi^+ \otimes \phi^+ \otimes \varphi^+$ evolves as follows,

$$\begin{aligned}
 &(\Psi^+ \otimes \phi^+ \otimes \varphi^+)_{AB} \\
 &= \frac{1}{2\sqrt{2}}[(|HV\rangle + |VH\rangle) \otimes (|II\rangle + |EE\rangle) \\
 &\quad \otimes (|lr\rangle + |rl\rangle)]_{AB} \\
 &\xrightarrow{\text{PBS } 0^\circ} \frac{1}{2\sqrt{2}}(|HV\rangle + |VH\rangle) \\
 &\quad \otimes (|I_A I_B\rangle + |I_r A I_r B\rangle + |E_L A E_L B\rangle + |E_r A E_r B\rangle) \\
 &\xrightarrow{\text{BS}} \frac{1}{2\sqrt{2}}|HV\rangle \otimes (|I_A I_A\rangle - |I_B I_B\rangle) \\
 &\quad + |I_r A I_r A\rangle - |I_r B I_r B\rangle + |E_L A E_L A\rangle \\
 &\quad - |E_L B E_L B\rangle + |E_r A E_r A\rangle - |E_r B E_r B\rangle) \\
 &\xrightarrow{\text{PBS } 0^\circ} \frac{1}{2\sqrt{2}}|HV\rangle \otimes (|B_l C_l\rangle - |C_l B_l\rangle + |D_l A_l\rangle \\
 &\quad - |A_l D_l\rangle + |B_r C_r\rangle - |C_r B_r\rangle \\
 &\quad + |D_r A_r\rangle - |A_r D_r\rangle) \\
 &\xrightarrow{\text{PBS } 45^\circ} \frac{1}{2\sqrt{2}}(|B_l^- C_l^+\rangle - |B_l^+ C_l^-\rangle + |B_r^- C_r^+\rangle \\
 &\quad - |B_r^+ C_r^-\rangle + |D_l^- A_l^+\rangle - |D_l^+ A_l^-\rangle \\
 &\quad + |D_r^- A_r^+\rangle - |D_r^+ A_r^-\rangle). \quad (6)
 \end{aligned}$$

This is the fifth group in Table I, which shows the relations between Alice's operations and Bob's detections. Here, the 16 states are divided into 12 distinct classes according to the detector outcomes. Here, the subscript “+” indicates the port associated with transmission through the PBS and “-” the port with reflection. Four of the classes contain two states each, and all eight other classes each contains exactly one state. Thus, with our protocol, this hyperentangled state can be used for

TABLE I. Detection outcome table. The 16 hyperentangled Bell states are detected using the state $|\varphi^+\rangle$ of the third DOF as an ancilla. “+” and “-” represent two detectors of each output port, respectively.

| | U_{ij} | State | Detector outcomes |
|----|------------------------------|-------------------------|--|
| 1 | $\sigma_2 \otimes \sigma'_3$ | $\Psi^+ \otimes \psi^-$ | $A_r^+ A_r^+, A_l^+ A_l^+, B_r^+ B_r^+, B_l^+ B_l^+$ |
| | $\sigma_3 \otimes \sigma'_2$ | $\Psi^- \otimes \psi^+$ | $C_r^+ C_r^+, C_l^+ C_l^+, D_r^+ D_r^+, D_l^+ D_l^+$ $A_r^- A_r^-, A_l^- A_l^-, B_r^- B_r^-, B_l^- B_l^-$ $C_r^- C_r^-, C_l^- C_l^-, D_r^- D_r^-, D_l^- D_l^-$ |
| 2 | $\sigma_0 \otimes \sigma'_0$ | $\Phi^+ \otimes \phi^+$ | $A_r^+ A_l^-, A_r^- A_l^+, B_r^+ B_l^-, B_r^- B_l^+$ |
| | $\sigma_1 \otimes \sigma'_1$ | $\Phi^- \otimes \phi^-$ | $C_r^+ C_l^-, C_r^- C_l^+, D_r^+ D_l^-, D_r^- D_l^+$ |
| 3 | $\sigma_1 \otimes \sigma'_0$ | $\Phi^- \otimes \phi^+$ | $A_r^+ A_l^+, A_r^- A_l^-, B_r^+ B_l^+, B_r^- B_l^-$ |
| | $\sigma_0 \otimes \sigma'_1$ | $\Phi^+ \otimes \phi^-$ | $C_r^+ C_l^+, C_r^- C_l^-, D_r^+ D_l^+, D_r^- D_l^-$ |
| 4 | $\sigma_3 \otimes \sigma'_3$ | $\Psi^- \otimes \psi^-$ | $A_r^+ B_r^-, A_r^- B_r^+, C_r^+ D_r^-, C_r^- D_r^+$ |
| | $\sigma_2 \otimes \sigma'_2$ | $\Psi^+ \otimes \psi^+$ | $A_l^+ B_l^-, A_l^- B_l^+, C_l^+ D_l^-, C_l^- D_l^+$ |
| 5 | $\sigma_2 \otimes \sigma'_0$ | $\Psi^+ \otimes \phi^+$ | $A_r^+ D_r^-, A_r^- D_r^+, C_r^+ B_r^-, C_r^- B_r^+$ |
| | | | $A_l^+ D_l^-, A_l^- D_l^+, C_l^+ B_l^-, C_l^- B_l^+$ |
| 6 | $\sigma_0 \otimes \sigma'_3$ | $\Phi^+ \otimes \psi^-$ | $A_r^+ D_l^+, A_r^- D_l^-, C_r^+ B_l^+, C_r^- B_l^-$ |
| | | | $A_l^+ D_r^+, A_l^- D_r^-, C_l^+ B_r^+, C_l^- B_r^-$ |
| 7 | $\sigma_2 \otimes \sigma'_1$ | $\Psi^+ \otimes \phi^-$ | $A_r^+ D_r^+, A_r^- D_r^-, C_r^+ B_r^+, C_r^- B_r^-$ |
| | | | $A_l^+ D_l^+, A_l^- D_l^-, C_l^+ B_l^+, C_l^- B_l^-$ |
| 8 | $\sigma_1 \otimes \sigma'_3$ | $\Phi^- \otimes \psi^-$ | $A_r^+ D_l^-, A_r^- D_l^+, C_r^+ B_l^-, C_r^- B_l^+$ |
| | | | $A_l^+ D_r^-, A_l^- D_r^+, C_l^+ B_r^-, C_l^- B_r^+$ |
| 9 | $\sigma_3 \otimes \sigma'_0$ | $\Psi^- \otimes \phi^+$ | $A_r^+ C_r^+, A_r^- C_r^-, B_r^+ D_r^+, B_r^- D_r^-$ |
| | | | $A_l^+ C_l^+, A_l^- C_l^-, B_l^+ D_l^+, B_l^- D_l^-$ |
| 10 | $\sigma_0 \otimes \sigma'_2$ | $\Phi^+ \otimes \psi^+$ | $A_r^+ C_l^-, A_r^- C_l^+, B_r^+ D_r^-, B_r^- D_r^+$ |
| | | | $A_l^+ C_r^-, A_l^- C_r^+, B_l^+ D_r^-, B_l^- D_r^+$ |
| 11 | $\sigma_3 \otimes \sigma'_1$ | $\Psi^- \otimes \phi^-$ | $A_r^+ C_r^-, A_r^- C_r^+, B_r^+ D_r^-, B_r^- D_r^+$ |
| | | | $A_l^+ C_l^-, A_l^- C_l^+, B_l^+ D_l^-, B_l^- D_l^+$ |
| 12 | $\sigma_1 \otimes \sigma'_2$ | $\Phi^- \otimes \psi^+$ | $A_r^+ C_l^+, A_r^- C_l^-, B_r^+ D_l^+, B_r^- D_l^-$ |
| | | | $A_l^+ C_r^+, A_l^- C_r^-, B_l^+ D_r^+, B_l^- D_r^-$ |

hyperdense coding to transmit $\log_2 12 = 3.58$ bits of classical information by sending one photon. As shown in Table I, photon-number resolving detectors [28] are required to detect the hyperentangled state in the first group. Otherwise, the classical information per photon decreases to $\log_2 11 = 3.45$ bits. Here, we have used current experimentally available hyperentangled states to demonstrate the principle of our hyperdense coding protocol. Similar schemes can be designed with other kinds of hyperentangled states as well.

III. HYPERENTANGLED BELL-STATE ANALYSIS ASSISTED BY AUXILIARY ENTANGLEMENT

We have demonstrated the analysis of two-DOF hyperentangled Bell states with the help of an auxiliary known entangled state. It is natural, therefore, to ask to what extent additional auxiliary entangled states can help in the HBSA of n -DOF hyperentangled Bell states and how many auxiliary entangled states are required to realize the full HBSA. We first review the entangled state analysis and then investigate the principle of HBSA assisted by auxiliary entanglement.

To distinguish the four 2-qubit Bell states is to identify two bits of information—the parity information represented by “ Ψ ” or “ Φ ” and the phase information denoted by “ \pm ” in Eqs. (2) and (3). Generally, we have two tools to get this information. The first one is projective measurement.

More specifically, two-photon product measurements in the computational basis can read the parity bit while measurements in the diagonal basis can get the phase information. However, these two bits of information cannot be obtained simultaneously. This makes complete BSA impossible with one copy of the state, but possible with two copies [25,27]. The other tool is the beam splitter, which interferes photons and distinguishes the antisymmetric state such as the singlet state $|\psi^-\rangle$ from the symmetric ones based on their symmetry property. Combining these two methods, four Bell states can be grouped into three classes, based on which $\log_2 3 \approx 1.58$ bits classical information could be transmitted via dense coding.

In 2003, Walborn *et al.* proposed a complete polarization BSA scheme without resorting to beam splitters as described above [15]. Instead, an additional spatial DOF was utilized. The parity information of the polarization entangled states was copied to the phase information of the spatial states by performing a controlled-NOT (CNOT) gate between these two DOFs of the same photon.

$$\begin{aligned} |\Phi^\pm\rangle|\psi^+\rangle &\xrightarrow{\text{CNOT}} |\Phi^\pm\rangle|\psi^+\rangle, \\ |\Psi^\pm\rangle|\psi^+\rangle &\xrightarrow{\text{CNOT}} |\Psi^\pm\rangle|\phi^+\rangle. \end{aligned} \quad (7)$$

Although the parity and phase information of Bell states in one DOF cannot be read at the same time, different DOFs can be measured simultaneously. Projective measurements of the polarization state in the diagonal basis and of the spatial mode in the computational basis allow discrimination of the four polarization Bell states.

The phase information of the polarization state can also be transferred to the spatial DOF in an equivalent way. As we know, the CNOT gate is difficult to accomplish between photons since a stable interaction at the single particle level is beyond current experimental capabilities [29]. However, a CNOT gate between different DOFs of the same photon is easy to execute with linear optics, such as PBS, BS, and so on. This provides a way to faithfully transfer information between different DOFs [30] and realize complete BSA with one extra entangled DOF. For Bell states in one DOF, a single auxiliary entangled state can help to realize full BSA. However, when the number of DOFs $n \geq 2$, the symmetry property should also be utilized to optimize distinguishing efficiency.

The generalized n -DOF hyperentangled Bell state can be viewed as the tensor product of Bell states of each DOF, $\prod_i^n |\Omega\rangle_i$, where the subscript i denotes the i th DOF, and $|\Omega\rangle$ can be one of the four Bell states of each DOF ($\Omega \in \{|\phi^+\rangle, |\phi^-\rangle, |\psi^+\rangle, |\psi^-\rangle\}$). For n two-state variables, there are 4^n mutually orthogonal hyperentangled states. The principle of HBSA is the same as that of BSA. We can use projective measurements to read parity or phase information and use beam splitters to distinguish antisymmetric states from symmetric ones. In our hyperdense coding scheme, the parity information of the polarization DOF was transferred to the momentum DOF through the effect of PBSs, which increased the number of distinct groups from $x_0(2) = 7$ to 12. For simplicity, we read the parity information of each DOF with projective measurements and transfer the phase information to the parity information of the auxiliary entangled states. By measuring each DOF in the computational basis to read the parity information, 4^n states can be classified into 2^n groups.

States in one group have the same order of $|\psi\rangle$ and $|\phi\rangle$, but different phase “ \pm .” Therefore, each group has 2^n states. As the singlet state $|\psi^-\rangle$ is antisymmetric while the triplet states are symmetric, $2^n - 1$ groups can be further divided into two according to the parity of the number of $|\psi^-\rangle$ states in these n DOFs. There is a special group in which all DOFs are in the $|\phi\rangle$ state, which cannot be further segmented based on symmetry. To sum up, with linear optics, 4^n states can be separated into x_0 groups,

$$x_0(n) = (2^n - 1) * 2 + 1 = 2^{n+1} - 1. \quad (8)$$

Here, one group is composed of 2^n different states ($|\phi^\pm\rangle^{\otimes n}$) and the other $2^{n+1} - 2$ groups each have 2^{n-1} states [27].

Auxiliary entanglement can enhance the distinguishability of states in HBSA. We now deduce step by step the number of distinct groups that are possible using k additional known entangled states. Based on the structure of the groups we can obtain from linear optics, the purpose of additional entanglement is to extract the phase information of each DOF of the hyperentangled Bell state, via computational basis measurements on the ancilla. Suppose for n -DOF hyperentangled Bell states, one additional entangled state $|\psi^+\rangle_{1'}$ is introduced. Then the joint $(n+1)$ -DOF state of the two photons is $\prod_{i=1}^n |\Omega\rangle_i \otimes |\psi^+\rangle_{1'}$ ($\Omega \in \{|\phi^+\rangle, |\phi^-\rangle, |\psi^+\rangle, |\psi^-\rangle\}$). We then copy the phase information of the first DOF $|\Omega\rangle_1$ to the parity of the auxiliary entangled state, which can be read out by projective measurements of the auxiliary DOF in the computational basis. We know the Bell states of the first DOF have two different possible phases in $(2^{n+1} - 3)$ of the groups obtained using linear optics. Each of these groups can be divided into two groups using the measurement outcome of the auxiliary entangled state, i.e., odd (even) parity of the additional DOF stands for the “+” (“-”) phase of the first DOF. However, there are two groups in which the first DOF is in the states $|\psi^+\rangle_1$ or $|\psi^-\rangle_1$. The 2^{n-1} states in these two groups can be written as $|\psi^+\rangle_1 \otimes \prod_{i=2}^n |\phi^\pm\rangle_i$ or $|\psi^-\rangle_1 \otimes \prod_{i=2}^n |\phi^\pm\rangle_i$, which cannot be further segmented with the help of the additional entanglement. To sum up, with one extra entangled state, there are $x_1(n) = 2^{n+2} - 4$ distinguishable groups. For example, we get $x_1(2) = 12$ groups in our hyperdense coding scheme.

Better results can be obtained by increasing the number of additional entangled states. Each time we increase the number of auxiliary entangled states by one, more groups can be obtained by subdividing the existing groups. Suppose there are k auxiliary entangled states. Then the overall state is $\prod_{i=1}^n |\Omega\rangle_i \otimes \prod_{i'=1}^k |\psi^+\rangle_{i'}$. We use the i' th additional entanglement to copy the phase information of the i th DOF to be distinguished, with which groups can be further divided. The ability for subdividing is based on the structure of groups without any auxiliary. If the second auxiliary entangled state $|\psi^+\rangle_{2'}$ is introduced, there are $2^{n+2} - 12$ groups that each can be divided into two groups based on the phase information of the second DOF while there are eight groups that cannot be subdivided. In these groups, the second DOF is in $|\psi^+\rangle$ or $|\psi^-\rangle$ state while the third, fourth, \dots , n th DOFs are all in the $|\phi^\pm\rangle$ states. Similarly, with k additional entangled states, more groups can be achieved on the basis of the $k - 1$ distinguishability. The groups that cannot be further divided are those with the k th DOF in the $|\psi^+\rangle$ or $|\psi^-\rangle$ state and the

$(k+1)$ th, $(k+2)$ th, \dots , n th DOFs all in the $|\phi^\pm\rangle$ state. The number of those groups is y_k ,

$$y_k = 2^k (C_{k-1}^0 + C_{k-1}^1 + \dots + C_{k-1}^{k-1}). \quad (9)$$

Therefore, with k additional entangled states, the number of distinguishable groups we obtain is

$$\begin{aligned} x_k &= 2(x_{k-1} - y_k) + y_k \\ &= 2x_{k-1} - 2^k (C_{k-1}^0 + C_{k-1}^1 + \dots + C_{k-1}^{k-1}) \\ &= 2x_{k-1} - 2^{2k-1} \quad (k = 1, 2, 3, \dots, n). \end{aligned} \quad (10)$$

Since $x_0(n) = 2^{n+1} - 1$, we obtain $x_k(n) = 2^{n+k+1} - 2^{2k}$. This means that with k entangled auxiliaries, $2^{n+k+1} - 2^{2k}$ groups out of 4^n states can be distinguished. Moreover, it shows that full HBSA requires $k = n$ additional auxiliary entangled states since $x_n = 4^n$.

IV. DISCUSSION AND SUMMARY

In this Rapid Communication, we have described a method for HBSA based on linear optics and ancilla entanglement, and have used our method to propose a hyperdense coding scheme using a two-photon six-qubit hyperentangled state. Without resorting to nonlinear interactions, our scheme achieves a 3.58 bits/photon classical information transmission rate, which outperforms the best schemes using linear optics. The key component of our hyperdense coding protocol is the HBSA. The hyperentangled Bell states in the first two DOFs are distinguished with the help of the known auxiliary entanglement in the third DOF. In our scheme, 16 states are separated into 12 groups, which is more than the seven groups created in previous schemes. Moreover, eight of the 12 groups only have one state, which means these eight hyperentangled states are unambiguously identified. Although our HBSA scheme cannot perfectly implement quantum teleportation, it may be used in a postselective way by probabilistically entangling the auxiliary DOF of the two photons before performing the HBSA. Previous protocols have divided the 64 hyperentangled Bell states in all the three DOFs into 15 groups [27]. Although this can increase the information transmission rate in hyperdense coding, it requires the sender to be capable of performing 64 unitary operations, which is much more than the 16 operations required in our present scheme.

We have analyzed the distinguishability of HBSA assisted by auxiliary entanglement for the general case of n DOF. The difficulty of performing complete BSA and HBSA lies in the inability to read both the parity and phase information at the same time. Therefore, additional resources such as nonlinear interactions or enlarged Hilbert spaces are utilized to improve the distinguishability. Although complete HBSA can be realized with the help of nonlinear effects via the use of coherent states [20] or a quantum dot cavity [21,22], these nonlinear interactions are actually too weak to realize with current technology. Our scheme also utilizes auxiliary resources to extract more information. However, no additional photons, coherent states, quantum dots, or other nonlinear interactions are required. Moreover, our hyperdense coding scheme can be implemented with hyperentangled states that can be generated with current technology. Two-qubit gates

between different DOFs can be implemented with only simple linear optics, which makes our scheme simpler to implement.

In summary, we have proposed a HBSA protocol assisted by auxiliary entanglement and have derived a formula to calculate the number of distinct groups of hyperentangled states distinguishable with the help of k additional entangled states. For states hyperentangled in n DOF, complete HBSA is achievable when $k = n$. Our scheme only requires linear optics, which makes it more practical and efficient for applications such as quantum hyperdense coding to expand the channel capacity,

and for other quantum information processing protocols requiring hyperentangled Bell-state analysis.

ACKNOWLEDGMENTS

X.L. is supported by the National Natural Science Foundation of China under Grants No. 11574038 and No. 11547305. S.G. acknowledges support from the Natural Sciences and Engineering Research Council of Canada.

-
- [1] C. H. Bennett, G. Brassard, C. Crepeau, R. Jozsa, A. Peres, and W. K. Wootters, Teleporting an Unknown Quantum State via Dual Classical and Einstein-Podolsky-Rosen Channels, *Phys. Rev. Lett.* **70**, 1895 (1993).
- [2] C. H. Bennett and S. J. Wiesner, Communication via One- and Two-Particle Operators on Einstein-Podolsky-Rosen States, *Phys. Rev. Lett.* **69**, 2881 (1992).
- [3] X. S. Liu, G. L. Long, D. M. Tong, and L. Feng, General scheme for superdense coding between multiparties, *Phys. Rev. A* **65**, 022304 (2002).
- [4] M. Zukowski, A. Zeilinger, M. A. Horne, and A. K. Ekert, Event-Ready-Detectors Bell Experiment via Entanglement Swapping, *Phys. Rev. Lett.* **71**, 4287 (1993).
- [5] H.-J. Briegel, W. Dür, J. I. Cirac, and P. Zoller, Quantum Repeaters: The Role of Imperfect Local Operations in Quantum Communication, *Phys. Rev. Lett.* **81**, 5932 (1998).
- [6] P. G. Kwiat, Hyper-entangled states, *J. Mod. Opt.* **44**, 2173 (1997).
- [7] J. T. Barreiro, N. K. Langford, N. A. Peters, and P. G. Kwiat, Generation of Hyperentangled Photon Pairs, *Phys. Rev. Lett.* **95**, 260501 (2005).
- [8] G. Vallone, R. Ceccarelli, F. De Martini, and P. Mataloni, Hyperentanglement of two photons in three degrees of freedom, *Phys. Rev. A* **79**, 030301(R) (2009).
- [9] N. Lütkenhaus, J. Calsamiglia, and K.-A. Suominen, Bell measurements for teleportation, *Phys. Rev. A* **59**, 3295 (1999).
- [10] L. Vaidman and N. Yoran, Methods for reliable teleportation, *Phys. Rev. A* **59**, 116 (1999).
- [11] J. Calsamiglia and N. Lütkenhaus, Maximum efficiency of a linear-optical Bell-state analyzer, *Appl. Phys. B: Lasers Opt.* **72**, 67 (2001).
- [12] S. Ghosh, G. Kar, A. Roy, A. Sen(De), and U. Sen, Distinguishability of Bell States, *Phys. Rev. Lett.* **87**, 277902 (2001).
- [13] J. Calsamiglia, Generalized measurements by linear elements, *Phys. Rev. A* **65**, 030301 (2002).
- [14] P. G. Kwiat and H. Weinfurter, Embedded Bell state analysis, *Phys. Rev. A* **58**, R2623 (1998).
- [15] S. P. Walborn, S. Padua, and C. H. Monken, Hyperentanglement-assisted Bell-state analysis, *Phys. Rev. A* **68**, 042313 (2003).
- [16] C. Schuck, G. Huber, C. Kurtsiefer, and H. Weinfurter, Complete Deterministic Linear Optics Bell State Analysis, *Phys. Rev. Lett.* **96**, 190501 (2006).
- [17] M. Barbieri, G. Vallone, P. Mataloni, and F. De Martini, Complete and deterministic discrimination of polarization Bell states assisted by momentum entanglement, *Phys. Rev. A* **75**, 042317 (2007).
- [18] X. F. Ren, G. P. Guo, and G. C. Guo, Complete Bell-states analysis using hyper-entanglement, *Phys. Lett. A* **343**, 8 (2005).
- [19] B. P. Williams, R. J. Sadler, and T. S. Humble, Superdense Coding over Optical Fiber Links with Complete Bell-State Measurements, *Phys. Rev. Lett.* **118**, 050501 (2017).
- [20] Y. B. Sheng, F. G. Deng, and G. L. Long, Complete hyperentangled-Bell-state analysis for quantum communication, *Phys. Rev. A* **82**, 032318 (2010).
- [21] B. C. Ren, H. R. Wei, M. Hua, T. Li, and F. G. Deng, Complete hyperentangled-Bell-state analysis for photon systems assisted by quantum-dot spins in optical microcavities, *Opt. Express* **20**, 24664 (2012).
- [22] T. J. Wang, Y. Lu, and G. L. Long, Generation and complete analysis of the hyperentangled Bell state for photons assisted by quantum-dot spins in optical microcavities, *Phys. Rev. A* **86**, 042337 (2012).
- [23] X. H. Li and S. Ghose, Self-assisted complete maximally hyperentangled state analysis via the cross-Kerr nonlinearity, *Phys. Rev. A* **93**, 022302 (2016).
- [24] X. H. Li and S. Ghose, Complete hyperentangled Bell state analysis for polarization and time-bin hyperentanglement, *Opt. Express* **24**, 18388 (2016).
- [25] T. C. Wei, J. T. Barreiro, and P. G. Kwiat, Hyperentangled Bell state analysis, *Phys. Rev. A* **75**, 060305 (2007).
- [26] T. M. Graham, C. K. Zeidler, and P. G. Kwiat, Quantum hyperdense coding, in *Frontiers in Optics 2015*, OSA Technical Digest (online) (Optical Society of America, Washington, DC, 2015), paper FTh3D.4.
- [27] N. Pinti, C. P. E. Gaebler, and T. W. Lynn, Distinguishability of hyperentangled Bell states by linear evolution and local projective measurement, *Phys. Rev. A* **84**, 022340 (2011).
- [28] B. E. Kardynał, Z. L. Yuan, and A. J. Shields, An avalanche-photodiode-based photon-number-resolving detector, *Nat. Photon.* **2**, 425 (2008).
- [29] J. L. O'Brien, G. J. Pryde, A. G. White, T. C. Ralph, and D. Branning, Demonstration of an all-optical quantum controlled-NOT gate, *Nature (London)* **426**, 264 (2003).
- [30] L. P. Deng, H. B. Wang, and K. G. Wang, Quantum CNOT gates with orbital angular momentum and polarization of single-photon quantum logic, *J. Opt. Soc. Am. B* **24**, 2517 (2007).